

The *C. elegans* RSA Complex Localizes Protein Phosphatase 2A to Centrosomes and Regulates Mitotic Spindle Assembly

Anne-Lore Schlaitz,¹ Martin Srayko,^{1,6,4} Alexander Dammermann,^{2,6} Sophie Quintin,^{1,6,5} Natalie Wielsch,¹ Ian MacLeod,³ Quentin de Robillard,¹ Andrea Zinke,¹ John R. Yates, III,³ Thomas Müller-Reichert,¹ Andrei Shevchenko,¹ Karen Oegema,² and Anthony A. Hyman^{1,*}

¹Max-Planck-Institute of Molecular Cell Biology and Genetics (MPI-CBG), Pfotenhauerstrasse 108, 01307 Dresden, Germany

²Department of Cellular and Molecular Medicine, Ludwig Institute for Cancer Research, School of Medicine, University of California, San Diego, La Jolla, CA 92093, USA

³Department of Cell Biology, The Scripps Research Institute, La Jolla, CA 92037, USA

⁴Present address: Department of Biological Sciences, University of Alberta, Edmonton, Alberta T6G 2E9, Canada.

⁵Present address: Institut de Génétique et de Biologie Moléculaire et Cellulaire, 1 rue Laurent Fries, BP 10142, 67404 Illkirch Cedex, France.

⁶These authors contributed equally to this work.

*Correspondence: hyman@mpi-cbg.de

DOI 10.1016/j.cell.2006.10.050

SUMMARY

Microtubule behavior changes during the cell cycle and during spindle assembly. However, it remains unclear how these changes are regulated and coordinated. We describe a complex that targets the Protein Phosphatase 2A holoenzyme (PP2A) to centrosomes in *C. elegans* embryos. This complex includes Regulator of Spindle Assembly 1 (RSA-1), a targeting subunit for PP2A, and RSA-2, a protein that binds and recruits RSA-1 to centrosomes. In contrast to the multiple functions of the PP2A catalytic subunit, RSA-1 and RSA-2 are specifically required for microtubule outgrowth from centrosomes and for spindle assembly. The centrosomally localized RSA-PP2A complex mediates these functions in part by regulating two critical mitotic effectors: the microtubule destabilizer KLP-7 and the *C. elegans* regulator of spindle assembly TPXL-1. By regulating a subset of PP2A functions at the centrosome, the RSA complex could therefore provide a means of coordinating microtubule outgrowth from centrosomes and kinetochore microtubule stability during mitotic spindle assembly.

INTRODUCTION

A mitotic spindle is a bipolar microtubule-based structure that ensures accurate inheritance of genetic material. As cells enter mitosis, the interphase microtubule cytoskeleton is reorganized to form the mitotic spindle. During spin-

dle formation, microtubule dynamics are modulated globally but also locally at spindle poles and in the vicinity of chromatin (Desai and Mitchison, 1997; Karsenti and Vernos, 2001; Wittmann et al., 2001). Numerous studies have shown that the function of many organizers of the microtubule cytoskeleton, such as microtubule motors and microtubule-associated proteins (MAPs), is modulated by their phosphorylation state (Verde et al., 1990; Nigg, 2001; Cassimeris, 1999). A key question that remains poorly understood is how protein phosphorylation is regulated temporally and spatially during spindle assembly. Phosphorylation states are determined by the balanced activities of kinases and phosphatases. Mitotic kinases (Nigg, 2001) rely largely on consensus sequence motifs for substrate recognition; however, recent work suggests that kinase activation and targeting can also occur through specific adaptor proteins. Examples include TPX2, which leads to activation of Aurora A kinase and its binding to spindle microtubules (Gruss and Vernos, 2004) and the chromosomal passenger proteins INCENP and Survivin, which localize and activate Aurora B kinase (Carmena and Earnshaw, 2003).

Protein phosphatases, which counteract the activity of kinases, are also required for correct microtubule organization. Protein Phosphatase 2A (PP2A), for example, has been implicated in the regulation of microtubule dynamics during the cell cycle (Gliksman et al., 1992; Tournebise et al., 1997), and Protein Phosphatase 4 is required for centrosome maturation and function (Sumiyoshi et al., 2002). The dephosphorylation of substrates during mitosis is presumably as tightly controlled as the corresponding phosphorylation reactions. However, there are far fewer phosphatases than kinases present in eukaryotic cells, and unlike kinases, most phosphatases do not appear to target consensus sequence motifs. This implies a far more complex regulation of individual phosphatases,

and regulatory subunits are crucial for the activity as well as the specificity of phosphatases (Faux and Scott, 1996; Dagda et al., 2003; Arnold and Sears, 2006). PP2A, for instance, forms heterotrimeric complexes consisting of a catalytic C subunit and a structural A subunit (the core heterodimer) and a variable regulatory B subunit. The association of the core heterodimer with different B subunits can modulate phosphatase activity, localization, or substrate specificity (Janssens and Goris, 2001). However, little is known about how regulatory subunits determine phosphatase function during mitosis and how they themselves are regulated.

In *C. elegans* embryos, centrosomes dominate the spindle-assembly process (Hamill et al., 2002; Oegema and Hyman, 2006). Shortly before mitotic spindle assembly, microtubule levels at *C. elegans* centrosomes increase about 5-fold (Hannak et al., 2002). A subset of these microtubules attach to the holocentric kinetochores to form kinetochore microtubules. Genome-wide RNA interference (RNAi) screens and forward genetics have identified a number of centrosome-localized effectors required for spindle assembly (reviewed in Oegema and Hyman, 2006). Microtubule nucleation requires centrosomal core components and a trimeric γ -tubulin complex (Hannak et al., 2002). Plus-end growth of microtubules away from the centrosome depends on free tubulin and the activity of a complex of ZYG-9 (the *C. elegans* ortholog of the microtubule stabilizer XMAP215) and its activator TAC-1 (Srayko et al., 2005). The number of microtubules that grow out from centrosomes is limited by the activity of the microtubule depolymerizing kinesin KLP-7 (Srayko et al., 2005). Proper length of kinetochore microtubules and therefore the stability of the assembling mitotic spindle depends on the activity of the Aurora A kinase AIR-1 and its activator TPXL-1 (Ozlu et al., 2005). However, it is still unclear how the process of spindle assembly is controlled temporally and spatially and how the different aspects of microtubule dynamics are coordinated to form this complex structure.

Here we identify a *C. elegans* protein complex that is required for two distinct processes in spindle formation: the outgrowth of microtubules from centrosomes and the stability of kinetochore microtubules. This complex consists of the new RSA-1 and RSA-2 proteins (Regulator of Spindle Assembly) and the core centrosomal protein SPD-5 and constitutes a centrosome-targeting module for Protein Phosphatase 2A.

RESULTS

The PP2A Regulatory Subunit RSA-1 Is Required for Spindle Stability and Normal Levels of Microtubules at Centrosomes

During a genome-wide RNA interference (RNAi) screen in *C. elegans* embryos, we identified C25A1.9, an uncharacterized gene whose silencing disrupted mitotic spindle assembly (Sonnichsen et al., 2005). Based on its RNAi phenotype and likely regulatory function (see below) we

termed C25A1.9 *rsa-1*, for regulator of spindle assembly. In *rsa-1(RNAi)* embryos, centrosomal microtubules were reduced (Figure 1A and Movie S1) and centrosomes collapsed onto chromatin after nuclear envelope breakdown (NEBD) and separated again at anaphase (Figures 1A and 1B). We used electron-microscope tomography to investigate the structure of the collapsed spindles more closely. Three-dimensional modeling of tomographic sections from *rsa-1(RNAi)* embryos with collapsed spindles showed that microtubules still contacted the chromatin (Figure 1D), suggesting that these spindles are otherwise intact and that kinetochore microtubules form but are less stable than in wild-type spindles.

We confirmed the *rsa-1(RNAi)* phenotype by isolating a mutant in *rsa-1* using ethyl-methane sulfonate (EMS) mutagenesis and TILLING to identify mutants in the gene (Figure S1; for a review of the TILLING method see Stemple, 2004). The mutant allele *rsa-1(dd13)*, predicted to give rise to a C-terminally truncated protein (Figures S1B and S1C), caused a phenotype indistinguishable from that of *rsa-1(RNAi)* embryos (Figure 1A and Movie S1).

RSA-1 encodes a 404 amino acid (aa) protein with sequence similarity to B-type regulatory subunits of Protein Phosphatase 2A (PP2A) (Figure S2). PP2A regulatory B subunits belong to one of at least three groups, the B, B', or B'' families (Janssens and Goris, 2001). Based on sequence conservation, the B'' subunits can be grouped into two classes: the PR48/PR130 and the TON2 subfamilies (Figure S2). RSA-1 is most closely related to B'' subunits of the TON2 subfamily (Figure S2). Consistent with this classification, the *Arabidopsis thaliana* B'' PP2A subunit TON2 has been implicated in aspects of microtubule cytoskeleton organization (Camilleri et al., 2002).

RSA-1 Is Part of a Complex that Contains the PP2A Core Heterodimer and a Previously Uncharacterized Protein, RSA-2

To test biochemically whether RSA-1 associates with a PP2A core heterodimer in *C. elegans*, we generated a worm strain expressing RSA-1 fused to green fluorescent protein (GFP) and immunoprecipitated the protein using anti-GFP antibodies. The *gfp::rsa-1* transgene fully rescued *rsa-1(dd13)* mutants, indicating that it is functional in vivo (see Supplemental Experimental Procedures). GFP::RSA-1 coprecipitated with the PP2A catalytic and structural subunits LET-92 and PAA-1, indicating that RSA-1 functions as part of a PP2A heterotrimeric complex. In addition to the PP2A core heterodimer, we consistently coimmunoprecipitated the core centrosomal protein SPD-5 and an uncharacterized protein, Y48A6B.11 (Table 1). SPD-5 is a coiled-coil protein required for the recruitment of all known components of the pericentriolar material (PCM) and thus is essential for the formation of functional centrosomes (Hamill et al., 2002; Dammermann et al., 2004). Nevertheless, no direct interaction partners of SPD-5 have been described to date. Y48A6B.11 is a coiled-coil-containing 108 kDa protein with no obvious

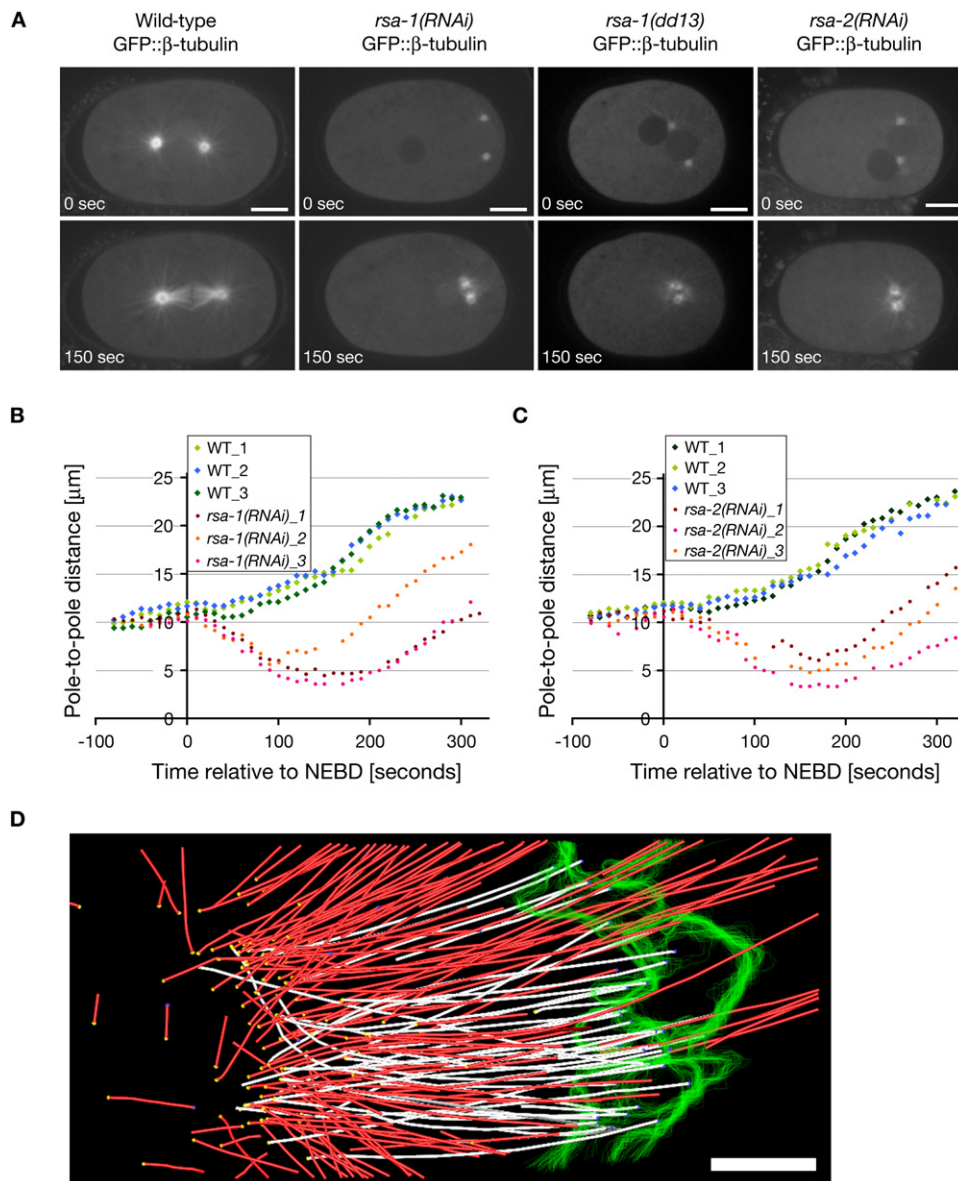


Figure 1. Spindle Assembly Fails in *C. elegans* Embryos Defective in the PP2A Regulatory Subunit RSA-1 and in Embryos Depleted of RSA-2

(A) Still images from spinning disk confocal time-lapse recordings of wild-type (first column), *rsa-1(RNAi)* (second column), *rsa-1(dd13)* (third column), and *rsa-2(RNAi)* (fourth column) one-cell stage *C. elegans* embryos expressing GFP:: β -tubulin. Time points are relative to nuclear envelope breakdown (NEBD = 0 s). Scale bars are 10 μm . See also [Movie S1](#).

(B and C) Measurement of pole-to-pole distances over time during spindle formation from single frames of time-lapse recordings as in (A). Measurements from three wild-type (WT) embryos (green and blue diamonds) and three *rsa-1(RNAi)* (B) or *rsa-2(RNAi)* (C) embryos (red and orange circles) are shown.

(D) Microtubules contacting the chromatin form in the absence of RSA-1. The 3D model shows a half spindle in anaphase. The partial reconstruction was computed from a 3×1 montage. The 3D model shows the boundaries of chromosomes (green) and the position of spindle microtubules (red and white lines). Microtubules that ended on the chromosomes were defined as kinetochore microtubules (white). Scale bar is 1 μm .

homologs in other organisms. *Y48A6B.11(RNAi)* embryos displayed a phenotype indistinguishable from that of *rsa-1(RNAi)* embryos ([Figures 1A and 1C](#) and [Movie S1](#)). Therefore, we refer to this gene as *rsa-2*.

A Targeting Pathway of SPD-5, RSA-2, and RSA-1 Recruits the PP2A Complex to Centrosomes

Consistent with the association of RSA-1 and RSA-2 with SPD-5, antibodies raised against these two proteins

Table 1. RSA-1 Coimmunoprecipitates with a PP2A Complex, SPD-5 and the Uncharacterized Protein Y48A6B.11 (RSA-2)

Proteins Coimmunoprecipitating Specifically with RSA-1	
Y48A6B.11 (RSA-2)	Uncharacterized protein. RNAi phenotype identical to <i>rsa-1(RNAi)</i>
SPD-5	Core component of the pericentriolar material
PAA-1	PP2A structural A subunit
LET-92	PP2A catalytic subunit

RSA-1 Coimmunoprecipitates with a PP2A Core Complex, SPD-5, and Y48A6B.11

Proteins coimmunoprecipitating with GFP::RSA-1 were separated by SDS-PAGE and analyzed by nanoLC-MS-MS. Corresponding molecular weight region samples of RSA-1 and control experiments were compared. Proteins that specifically coprecipitated with RSA-1 in two independent experiments are listed.

labeled centrosomes in wild-type embryos (Figure 2A), as did GFP fusions of the proteins (data not shown). The centrosomal staining was strongly reduced after RNAi knock-down of the respective proteins, confirming the specificity of the antibodies and the RNAi phenotypes (Figure 2A). In *spd-5(RNAi)* embryos, we could not detect any localized intracellular staining for RSA-1 or RSA-2, indicating that both proteins depend on SPD-5 for binding to centrosomes (data not shown).

In order to investigate the assembly relationship between RSA-1 and RSA-2, we determined the location of each protein in the absence of the other. In both *rsa-1(RNAi)* embryos (Figure 2A) and *rsa-1(dd13)* mutants (data not shown), RSA-2 localized correctly to centrosomes. However, in *rsa-2(RNAi)* embryos, RSA-1 was not detected on centrosomes (Figure 2A). Western blotting showed that RSA-1 levels were decreased by about 50% upon *rsa-2(RNAi)* and RSA-2 levels were also reduced by about 50% in *rsa-1(RNAi)* (Figure 2C). These results suggested that RSA-2 is specifically required for the centrosomal recruitment of RSA-1, while RSA-1 appears to be dispensable for RSA-2 binding to centrosomes.

A GFP-tagged version of the RSA-1-associated PP2A catalytic subunit LET-92 also localized to centrosomes. GFP::PP2Ac^{LET-92} fluorescence was additionally observed in the cytoplasm and around chromatin after NEBD. After depletion of RSA-1, the centrosomal GFP::PP2Ac^{LET-92} signal was no longer detectable, while the cytoplasmic and nuclear pools persisted (Figure 2B and Movie S2). These localization results suggested an assembly hierarchy of SPD-5, RSA-2, RSA-1, and the PP2A catalytic subunit onto centrosomes.

In order to investigate how the RSA proteins facilitate PP2A binding to centrosomes, we performed a yeast two-hybrid analysis. These experiments suggested that

RSA-2 could directly bind to both RSA-1 and the core PCM protein SPD-5 (Figure 2D and Table S1). Furthermore, we found that the amino-terminal part of RSA-2 interacted with SPD-5 and its carboxy-terminal half with RSA-1 (not shown), indicating that RSA-2 acts as a scaffold to link the phosphatase complex to centrosomes. These results support the view of a linear assembly pathway that is based on direct protein-protein interactions, whereby the centrosomal core protein SPD-5 links RSA-2 to centrosomes, which then recruits RSA-1, the localizing B regulatory subunit for the PP2A complex (Figure 2E).

RSA-1 and RSA-2 Are Required for the Generation of Normal Numbers of Outgrowing Microtubules from Centrosomes

To more closely examine the functions of RSA-1 and RSA-2, we measured centrosomal GFP:: β -tubulin fluorescence in *rsa-1(RNAi)* and *rsa-2(RNAi)* embryos. Centrosomal microtubules were reduced to 10%–20% of wild-type levels during prophase, and a small nonuniform accumulation of tubulin at centrosomes appeared after NEBD (Figures 3A–3D and Movie S1). Consistent with the microtubule reduction observed in *rsa-1(RNAi)* and *rsa-2(RNAi)* embryos, depletion of these proteins also caused a substantial decrease in outgrowth of microtubule plus ends from centrosomes (Movie S3). The number of microtubules growing out from *rsa-1(RNAi)* centrosomes at metaphase was previously measured to be approximately 25% of the wild-type number (Srayko et al., 2005).

Microtubule Stability at Centrosomes Depends on PP2A Catalytic Activity

To determine whether RSA-1- and RSA-2-mediated stabilization of centrosomal microtubules requires the PP2A catalytic subunit LET-92, we examined *let-92(RNAi)* embryos. In contrast to RSA-1 or RSA-2 depletion, *let-92(RNAi)* resulted in a highly pleiotropic phenotype, including a failure in meiotic spindle disassembly, a failure in the formation of nuclear envelopes around the pronuclei and unseparated centrosomes. Nevertheless, a spindle-like bipolar structure eventually formed (Figure 4A and Movie S4), but with greatly reduced microtubule numbers at the poles (Figure 4A, compare *let-92(RNAi)* panel IV with wild-type anaphase stage embryo in the right panel).

The pleiotropic defects observed in *let-92(RNAi)* embryos made it difficult to compare the function of this phosphatase with the functions of RSA-1 and RSA-2 in centrosomal microtubule stability. We therefore used the PP2A and Protein Phosphatase 1 (PP1) inhibitor Calyculin A to remove phosphatase activity from embryos that had progressed into mitosis normally. Embryos expressing YFP:: α -tubulin were mounted in the presence or absence of Calyculin A, which does not penetrate the eggshell. A UV laser was used to perforate the eggshell during

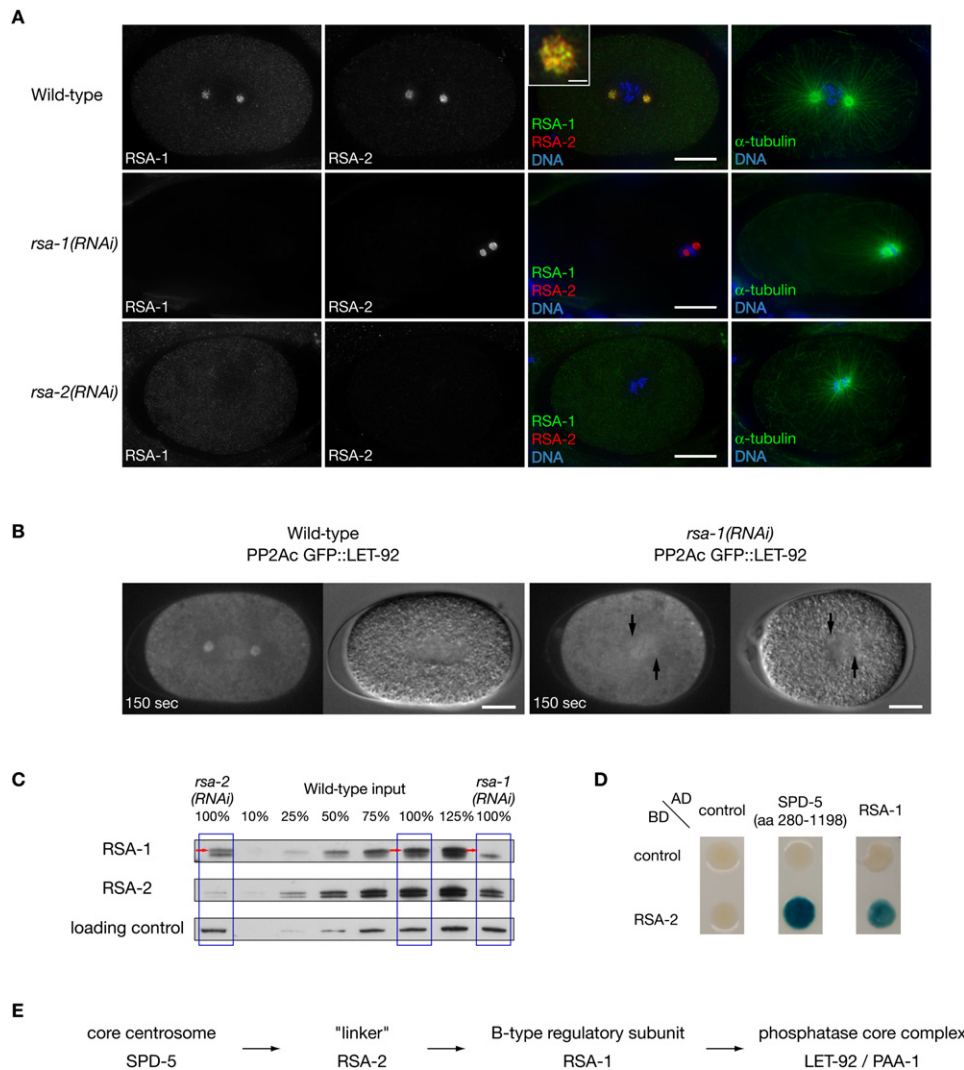


Figure 2. A Linear Assembly Hierarchy Targets the RSA-PP2A Complex to Centrosomes

(A) Centrosomal localization of RSA-1 depends on RSA-2. Wild-type, *rsa-1(RNAi)*, and *rsa-2(RNAi)* embryos were stained for DNA (blue), RSA-1 (green), RSA-2 (red), and microtubules (green in right panels). Projections of Z stacks are shown. The inset in the merged image of the top panel highlights RSA-1 and RSA-2 colocalization at centrosomes. Panels on the right illustrate the RNAi phenotypes and the position of the centrosomes. Scale bars are 10 μ m; inset scale bar is 1 μ m.

(B) The PP2A catalytic subunit LET-92 is recruited to centrosomes by RSA-1. Paired fluorescence and DIC still images from time-lapse series of metaphase embryos expressing the GFP-tagged PP2A catalytic subunit LET-92. A wild-type embryo is shown in the left panel, a *rsa-1(RNAi)* embryo is shown in the right panel. Arrows indicate the position of centrosomes in the *rsa-1(RNAi)* panel as obtained from corresponding DIC recordings. Times indicated are seconds relative to NEBD. Scale bars are 10 μ m. See [Movie S2](#).

(C) The mislocalization of RSA-1 in *rsa-2(RNAi)* does not appear to be caused by destabilization of the protein. Western blot of whole-worm lysates from wild-type, *rsa-1(RNAi)*, and *rsa-2(RNAi)* animals. Both the RSA-1 and the RSA-2 antibodies recognize a protein doublet. In the case of RSA-1, only the upper band (arrow) is specific for the protein, as the lower band is RNAi resistant. A nonspecific reactivity of the RSA-2 antibody served as loading control.

(D) RSA-2 interacts with RSA-1 and SPD-5 in a yeast two-hybrid assay. A vector encoding RSA-2 fused to the GAL4 DNA binding domain (BD) was cotransformed with GAL4 activating domain (AD) fusions of either full-length RSA-1 or a SPD-5 fragment that corresponded to aa 280–1198. Complex formation was detected by activation of the lacZ reporter gene in a β -galactosidase assay. See [Table S1](#) for a quantification of β -galactosidase units. Complex formation was further confirmed by use of two additional reporters: growth on plates lacking histidine or uracil, respectively (data not shown).

(E) Scheme of the linear assembly hierarchy that targets the PP2A complex to centrosomes.

mitosis, facilitating the entry of Calyculin A into the cytoplasm. In embryos exposed to Calyculin A, microtubules rapidly disappeared from centrosomes ([Figure 4B](#) and

[Movie S5](#)). These observations indicate that phosphatase catalytic activity is required for microtubule stability at spindle poles.

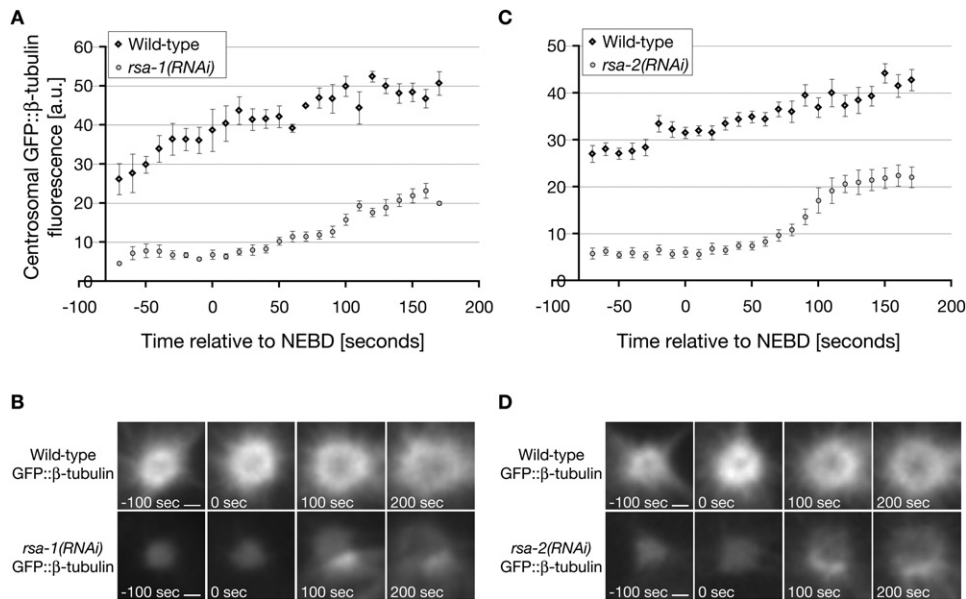


Figure 3. Depletion of RSA-1 or RSA-2 Causes a Reduction of Centrosomal Microtubules

(A and C) Quantification of centrosomal GFP::β-tubulin fluorescence from single frames of time-lapse recordings as in Figure 1A. Fluorescence intensity values are shown as (mean ± standard error of the mean) for wild-type (diamonds) and *rsa-1(RNAi)* (panel A) or *rsa-2(RNAi)* (panel C) embryos (circles).

(B and D) Representative images of centrosomes of *rsa-1(RNAi)* (panel B) and *rsa-2(RNAi)* (panel D) embryos acquired as in Figure 1A. Scale bars are 1 μm. Time points indicated are relative to NEBD.

RSA-1 and RSA-2 Control Microtubule Dynamics through the Microtubule Depolymerizing Kinesin KLP-7

Our results so far suggested that RSA-1 and RSA-2 mediate a specific subset of PP2A functions that are required for maintenance of normal microtubule levels at centrosomes. Microtubule amounts at *C. elegans* centrosomes are also modulated by KLP-7, the only identified Kinesin-13 in *C. elegans* (Desai et al., 1999; Siddiqui, 2002). However, in contrast to the RSA complex, which normally stabilizes microtubules, KLP-7 reduces the microtubule number at centrosomes. Specifically, the number of microtubule plus ends growing out from centrosomes is doubled in *klp-7(RNAi)* embryos (Srayko et al., 2005). Therefore, KLP-7 and the RSA complex have opposite effects on microtubule outgrowth. Indeed codepletion of KLP-7 and either RSA-1 or RSA-2 restored centrosomal microtubules to wild-type levels. However, spindle poles still collapsed onto each other (Figures 5A and 5B and Movies S6 and S7; for controls, see Experimental Procedures). Similar results were obtained when KLP-7 was depleted from *rsa-1(dd13)* mutant embryos (Figure S3 and Movie S8). Thus, codepletion of KLP-7 rescues the microtubule outgrowth defect in *rsa-1(RNAi)*, *rsa-1(dd13)*, and *rsa-2(RNAi)* embryos but cannot rescue spindle instability. This result indicates that the RSA complex has at least two functions in the formation of a mitotic spindle: regulation of kinetochore microtubule length and regulation of microtubule outgrowth from centrosomes. The above result also

suggested that the nucleation capacity of the centrosomes is intact in the absence of RSA-1 and RSA-2. Consistent with this notion, we found that γ-tubulin, the major microtubule nucleator in *C. elegans* embryos (Hannak et al., 2002), localizes normally in *rsa-1(RNAi)* and *rsa-2(RNAi)* embryos (Figures 5C, S4A, and S4B). We suggest that the RSA complex acts in a process downstream of microtubule nucleation per se and regulates the outgrowth of nucleated microtubules.

The RSA complex could control microtubule outgrowth from centrosomes directly by regulating KLP-7 catalytic activity, or indirectly, for instance by regulating KLP-7 levels at centrosomes. We tested whether the RSA-PP2A complex affects KLP-7 localization using a transgenic line expressing GFP-tagged KLP-7. KLP-7 levels at centrosomes were about 1.6–1.8-fold increased in *rsa-1(RNAi)*, as compared to wild-type (Figures 5D and 5E and Movie S9). This observation indicated that the RSA-PP2A complex controls microtubule outgrowth from centrosomes at least in part by restricting the levels of the microtubule destabilizer KLP-7 at centrosomes.

The RSA Complex Recruits the Kinetochore Microtubule Stabilizer TPXL-1 to Centrosomes

The collapse of spindle poles at NEBD and their subsequent re-elongation observed in *rsa-1(RNAi)* (Figures 1A and 1B and Movie S1) as well as the ultrastructure of *rsa-1(RNAi)* spindles obtained by EM tomography (Figure 1D) are very reminiscent of the depletion phenotype

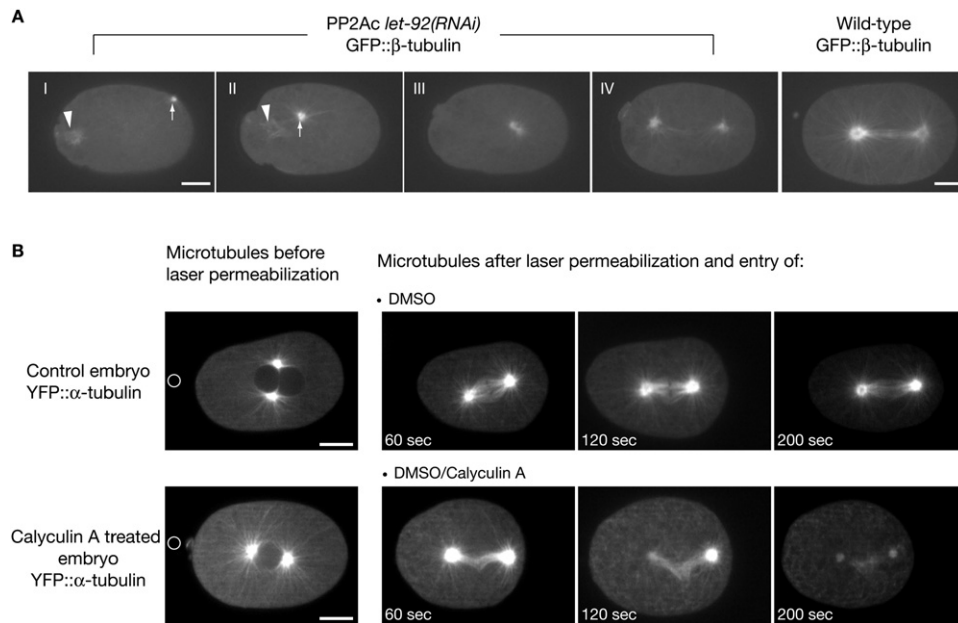


Figure 4. Protein Phosphatase Activity Is Required for Centrosomal Microtubule Stability

(A) Depletion of the PP2A catalytic subunit LET-92 leads to pleiotropic defects in the early embryo and to reduced centrosomal microtubules. Embryos expressing GFP:: β -tubulin were depleted of the PP2A catalytic subunit LET-92 and imaged by spinning disk confocal microscopy. Still images representing cell-cycle progression (panels I–IV) in *let-92(RNAi)* embryos are shown. In panel I, meiotic spindle remnants (arrowhead) and the unseparated centrosomes (arrow) are at the embryonic cortex. In panel II, meiotic spindle remnants and centrosomes migrate toward the center of the embryo where they meet. In panel III, the meiotic microtubule array and the centrosomes fuse and form a bipolar structure. In panel IV, the bipolar structure elongates. The right panel shows a still image of a wild-type embryo at anaphase acquired under the same conditions for comparison of microtubule amounts with panel IV of the *let-92(RNAi)* series. See [Movie S4](#).

(B) Microtubules are destabilized in embryos treated with Calyculin A, an inhibitor of Protein Phosphatase 2A and Protein Phosphatase 1. YFP:: α -tubulin embryos were mounted with 10 μ M Calyculin A diluted from a 1 mM DMSO stock (DMSO/Calyculin A embryo, lower panels) or with 1% v/v DMSO alone (DMSO control embryos, upper panels). An image of the cellular microtubules before drug treatment was acquired (left panels). After laser-mediated eggshell permeabilization and entry of Calyculin A into the embryonic cytoplasm (circle marks the site of eggshell perforation), microtubule behavior was followed using one-second interval time-lapse acquisitions. Time points indicated are seconds after eggshell perforation and drug entry (right panels). See [Movie S5](#).

Out of 15 embryos that were exposed to Calyculin A; 10 showed a rapid microtubule depolymerization like the embryo shown in this figure; 5 embryos displayed a slower loss of microtubules, which might be caused by slightly different cell-cycle stages at the time of drug entry or by poor access of Calyculin A to the cytoplasm of these embryos.

In panels (A) and (B), scale bars are 10 μ m.

described earlier for the Aurora kinase activator TPXL-1 ([Ozlu et al., 2005](#)), suggesting a role of the RSA complex in regulating TPXL-1.

Consistent with this idea, TPXL-1 amounts at centrosomes were substantially reduced after depletion of RSA-1 ([Figure 6A](#)). The decrease in TPXL-1 at the centrosome did not result from the reduced microtubule number, as it was also observed when microtubule amounts were restored to wild-type levels by codepletion of KLP-7 and RSA-1 ([Figures 6A and 6B](#) and [Movie S10](#)). Similar results were obtained in *rsa-2(RNAi)* (data not shown).

We next determined whether TPXL-1 and the RSA proteins also interact physically. Indeed, immunoprecipitation of TPXL-1 resulted in coprecipitation of the RSA complex, as judged by Western blot and mass spectrometry ([Figure 6C](#) and [Table S2](#)). Depletion of the RSA complex did not affect the localization of other known centrosomal regulators, (see [Figure S4](#)). Based on these results, we conclude that the RSA complex contributes to mitotic

spindle assembly, at least in part by targeting TPXL-1 to centrosomes, likely via a direct physical interaction.

DISCUSSION

PP2A Subunits and Specificity

One of the major questions regarding phosphatase regulation is how target specificity is achieved. Our data suggest that PP2Ac^{LET-92} activity in the *C. elegans* embryo is regulated by the RSA centrosome-targeting complex, indicating that the RSA complex confers temporal and spatial specificity to the PP2A holoenzyme. This result further suggests that other regulatory subunits could mediate different functions of PP2Ac^{LET-92} in the early embryo. Indeed, out of the potential PP2A subunits of the B, B', and B'' classes identified by BLAST searches (seven proteins in total), the B type subunit SUR-6 has a clear function in early embryonic mitoses ([Kao et al., 2004](#); [Sonnichsen et al., 2005](#); our unpublished observations). *sur-6(RNAi)*

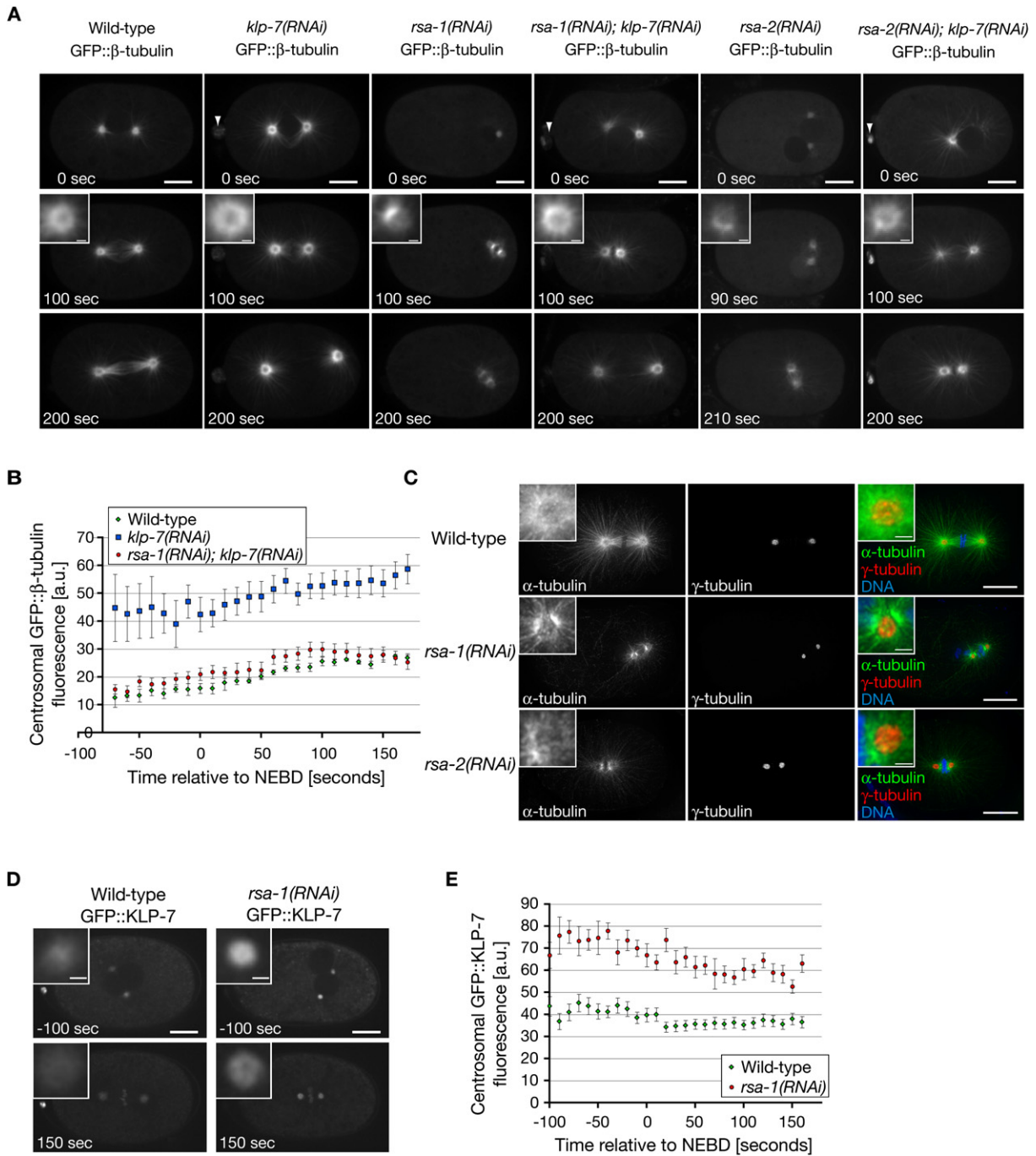


Figure 5. Microtubule Reduction in *rsa-1(RNAi)* and *rsa-2(RNAi)* Depends on KLP-7

(A) Microtubule reduction in *rsa-1(RNAi)* and *rsa-2(RNAi)* can be overcome by codepletion of the microtubule depolymerizing kinesin KLP-7. Shown are still images of time-lapse series of GFP:: β -tubulin-expressing embryos of wild-type, *klp-7(RNAi)*, and *rsa-1(RNAi)* single depletions, *rsa-1(RNAi); klp-7(RNAi)* double depletion as well as *rsa-2(RNAi)* single depletion and *rsa-2(RNAi); klp-7(RNAi)* double depletion. Aspects of both single depletion phenotypes are observable in the double RNAi experiments: spindle collapse marking *rsa-1(RNAi)* and *rsa-2(RNAi)*, respectively, and enlarged polar bodies (arrowheads), indicating efficient removal of KLP-7. Double RNAi experiments were controlled by dilution of single dsRNAs with an unspecific dsRNA. See [Movies S6 and S7](#).

(B) Quantification of centrosomal GFP:: β -tubulin fluorescence from single frames of time-lapse recordings as in (A). Measurements are displayed as (mean values \pm SEM) for wild-type embryos (green diamonds), *klp-7(RNAi)* embryos (blue squares) and *rsa-1(RNAi); klp-7(RNAi)* double RNAi embryos (red circles). Microtubule amounts for RSA-1 single depletion could not be quantified in this experiment, as exposure times had to be decreased to avoid overexposure of the brighter *klp-7(RNAi)* centrosomes, so that *rsa-1(RNAi)* centrosomes were too dim for quantifications. See [Figure 3A](#) for comparison of *rsa-1(RNAi)* and wild-type microtubule amounts.

did not alter the targeting of LET-92 or TPXL-1 to centrosomes (our unpublished observations). SUR-6, therefore, appears to mediate LET-92 functions that are separate from those regulated by RSA-1. The *Arabidopsis thaliana* homolog of RSA-1, TON2, is also required for microtubule organization (Camilleri et al., 2002). This raises the possibility that PP2A-B' subunits of the RSA-1/TON2 subfamily have a conserved role in the regulation of the microtubule cytoskeleton.

Apart from the roles of TON2 and the RSA complex, there is little evidence of specific PP2A complexes regulating microtubule functions in other organisms. A PP2A complex of defined subunit composition was observed to bind microtubules and centrosomes in mammalian tissue culture cells (Sontag et al., 1995). However, the mode of interaction of the respective B subunit with these structures was not determined, and the regulatory significance of this binding remains unclear.

Centrosomal Targeting of PP2A

The RSA complex contains a linker protein, RSA-2, which connects the core PCM protein SPD-5 to the PP2A complex via the B' subunit RSA-1. RSA-2 depletion caused no additional defects compared to RSA-1 depletion, and therefore it probably has no additional functions. RSA-2 might modulate the number of phosphatase complexes that bind to centrosomes or facilitate the presentation of substrates to the phosphatase and thereby adjust microtubule outgrowth to cellular needs. RSA-2 is the first identified target of the essential PCM recruiting protein SPD-5, and this interaction indicates that specific subcomplexes can be recruited by SPD-5, maybe via different domains of the protein. It will be interesting to determine how SPD-5 binds and recruits distinct proteins of the PCM.

Regulation of Microtubule Growth from Centrosomes through KLP-7 Targeting

Our data indicate that the RSA complex regulates microtubule growth from centrosomes through KLP-7. Recent work from our laboratory suggests that the Kinesin-13 proteins KLP-7 and MCAK limit the number of microtubules growing out from centrosomes, both in *C. elegans* embryos and in *Xenopus* egg extracts (Srayko et al., 2005; Kinoshita et al., 2005). As Kinesin-13 proteins are microtubule depolymerases that target microtubule ends, we presume that KLP-7 decreases the stability of nascent nucleated plus ends, although we cannot rule

out a role of KLP-7 in nucleation. Possibly, the RSA phosphatase complex regulates the catalytic activity of KLP-7 itself. Experiments in tissue culture cells have shown that phosphorylation decreases the microtubule depolymerizing activity of MCAK, the human homolog of KLP-7 (Andrews et al., 2004; Lan et al., 2004). By analogy, dephosphorylation by PP2A should increase the activity of KLP-7, contradictory to the apparent increase of KLP-7 activity after RNAi knockdown of the RSA complex. We cannot exclude that the RSA complex controls KLP-7 through a different phosphorylation site with an opposite effect on its enzymatic activity. However, our data suggest that the primary role of the RSA complex is the regulation of KLP-7 targeting. Consistent with this idea, a nonphosphorylatable mutant of *Xenopus laevis* MCAK cannot target to centromeres (Ohi et al., 2004).

Regulation of Spindle Formation by Targeting of the *C. elegans* Ortholog of TPX2

The most direct evidence we have found for how the RSA-PP2A complex regulates spindle assembly is through physical interaction with and targeting of TPXL-1 to centrosomes (Figures 6A–6C). Further support for the idea that TPXL-1 and the RSA complex work in the same pathway is that in both *tpxl-1(RNAi)* and *rsa-1(RNAi)* embryos, kinetochore microtubules form but are much shorter than in wild-type spindles (Ozlu et al., 2005 and Figure 1D).

C. elegans TPXL-1, like other microtubule-associated proteins, is highly basic and might thus bind to the acidic tails of tubulin. Phosphorylation is known to negatively regulate the binding of many MAPs to microtubules (Cassimeris and Spittle, 2001). It is conceivable that TPXL-1 is generally phosphorylated in *C. elegans* embryos and thereby prevented from binding to microtubules. Spatially restricted dephosphorylation at the centrosome by the RSA complex could enable TPXL-1 to bind microtubules and fulfill its microtubule-stabilizing function.

Coordination of Microtubule Outgrowth and Stability by the RSA Complex

One of the least explored problems in the assembly of complex cytoskeletal structures, like the mitotic spindle, is how the cell coordinates the distinct processes that lead to the formation of this structure. In this context, it is interesting that the RSA complex targets the appropriate amounts of two centrosome-effector proteins for correct spindle assembly. RSA-PP2A activity thereby potentially allows coordination of the different microtubule

(C) γ -tubulin localizes normally in *rsa-1(RNAi)* and *rsa-2(RNAi)* embryos. Wild-type, *rsa-1(RNAi)*, and *rsa-2(RNAi)* embryos were fixed and stained for DNA (blue), microtubules (green), and γ -tubulin (red). Z-stack projections are shown. See also Figure S4B for a quantification of γ -tubulin levels in *rsa-1(RNAi)*.

(D) Centrosomal levels of KLP-7 are increased in *rsa-1(RNAi)*. Shown are still images of time-lapse series of wild-type and *rsa-1(RNAi)* embryos expressing GFP::KLP-7. See also Movie S9.

(E) Quantification of centrosomal GFP::KLP-7 fluorescence in wild-type (WT) embryos (green diamonds) and *rsa-1(RNAi)* embryos (red circles) from single frames of time-lapse recordings as in panel (D). Values are mean \pm SEM. In panels (A) and (D), times indicated are seconds relative to NEBD. In panels (A), (C), and (D), scale bars are 10 μ m; inset scale bars are 1 μ m.

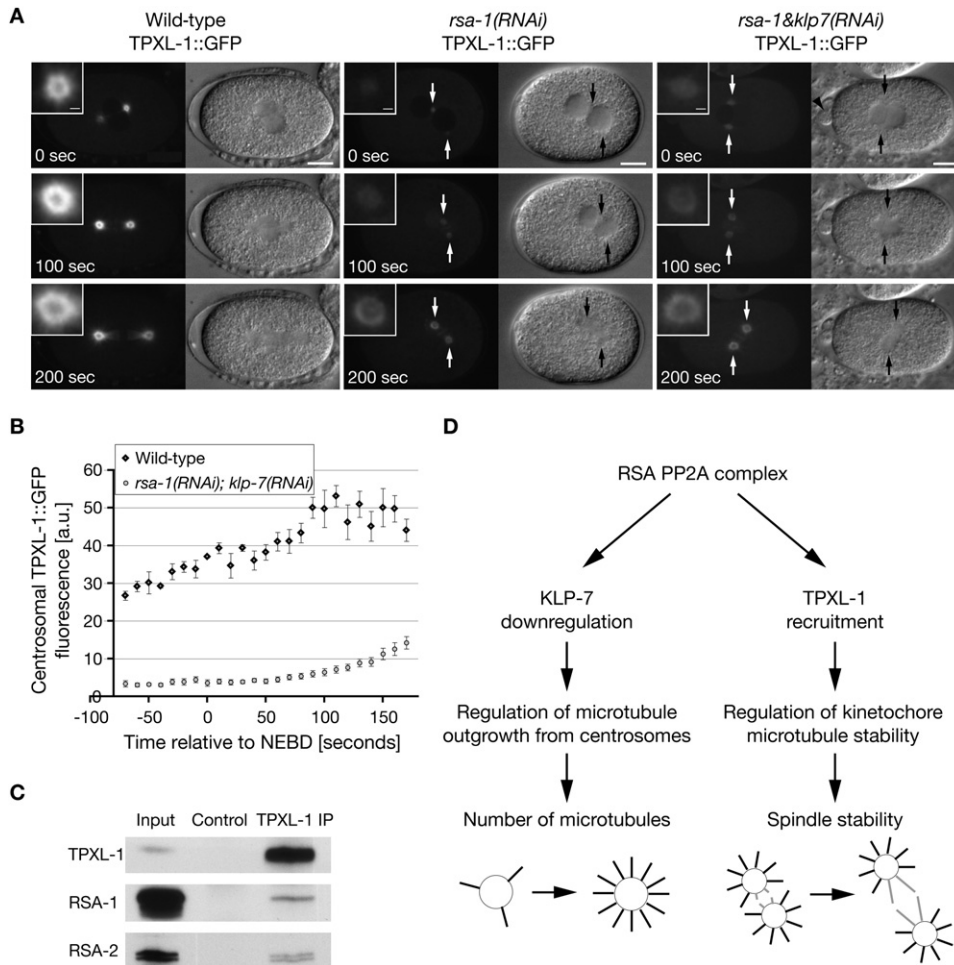


Figure 6. RSA-1 Is Required for the Centrosomal Localization of TPXL-1

(A) Shown are still images taken from time-lapse series of wild-type, *rsa-1(RNAi)*, and *rsa-1(RNAi); klp-7(RNAi)* double depletion embryos expressing TPXL-1::GFP. Paired fluorescence and DIC images are shown. Arrows indicate the positions of the centrosomes in *rsa-1(RNAi)* and *rsa-1(RNAi); klp-7(RNAi)*. Successful depletion of KLP-7 is indicated by an enlarged polar body (arrowhead). Time points are relative to NEBD. Scale bars are 10 μm. Inset scale bars are 1 μm. See [Movie S10](#).

(B) Quantification of centrosomal TPXL-1::GFP amounts from single frames of time-lapse recordings as shown in (A). Mean values ± SEM are shown for wild-type (green diamonds) and *rsa-1(RNAi); klp-7(RNAi)* centrosomes (circles).

(C) TPXL-1 associates with the RSA complex. TPXL-1 was immunoprecipitated from *C. elegans* embryo extracts. Copurifying proteins were identified by western blotting and antibody detection. In a different IP experiment, the association of TPXL-1 was confirmed by mass spectrometric analysis ([Table S2](#)).

(D) The RSA-PP2A Complex Regulates Two Separate Pathways in Spindle Formation. Downregulation of KLP-7 by RSA-PP2A allows the correct number of microtubules to grow out from centrosomes (left branch). Recruitment of TPXL-1 to centrosomes by the RSA-PP2A complex is required for stabilization of kinetochore microtubules (gray) and thereby spindle stability (right branch).

events required to form a spindle. By restricting the amount of KLP-7, the RSA complex ensures that enough microtubules grow from centrosomes to assemble a spindle. Concomitantly, recruitment of TPXL-1 by the RSA complex stabilizes some of these microtubules that are captured by kinetochores. The RSA complex could therefore integrate the requirements for microtubule stability at kinetochores and centrosomes, fine-tuning the number of microtubules contributing to the mitotic spindle accordingly.

EXPERIMENTAL PROCEDURES

Transgenic Worm Strains

All *C. elegans* strains were maintained as described ([Brenner, 1974](#)). Transgenic lines were created by microparticle bombardment as described ([Praitis et al., 2001](#)). The strains used are listed in [Table S3](#).

The isolation of mutant alleles by TILLING is outlined in the supplemental material section.

RNA-Mediated Interference (RNAi)

dsRNA synthesis was performed as previously described ([Oegema et al., 2001](#)) using N2 genomic DNA as template and the primer

sequences documented at <http://www.worm.mpi-cbg.de/phenobank2/cgi-bin/PrimersPage.py> (*rsa-1*, *rsa-2*, and *let-92* dsRNAs) and in Grill et al. (2001) (*klp-7* dsRNA).

The efficiency of depletion of each single protein in the double RNAi experiments was confirmed by dilution of specific dsRNAs with a dsRNA targeting MIG-5, a protein with no function in the one-cell stage embryo. Quantification of GFP:: β -tubulin fluorescence revealed that *rsa-1(RNAi)* and *rsa-1(RNAi); mig-5(RNAi)* caused an identical reduction in centrosomal microtubule levels (not shown). Reduction of the two depleted proteins in the double RNAi experiment was also confirmed by immunostaining. Primers for *mig-5* dsRNA production were AATTAACCTCACTAAAGGCAGTGGCCTCAAGCAGT (forward) and TAATACGACTCACTATAGCTGCCAGAGCATGTGGTG (reverse).

dsRNA was injected into the gonad of L4 stage hermaphrodites, and the worms were incubated at 25°C for 22–26 hr before being examined.

Time-Lapse Microscopy and Quantification

GFP:: β -tubulin, TPXL-1::GFP, GFP:: γ -tubulin and GFP::AIR-1 movies were acquired as described in Ozlu et al. (2005). For EBP-2::GFP, imaging was performed as described in Srayko et al. (2005). Quantification of centrosomal GFP:: β -tubulin, GFP:: γ -tubulin, GFP::KLP-7, and TPXL::GFP was performed with Metamorph Software. A circular region was used to measure fluorescence intensity at the centrosome and at a nearby cytoplasmic area ("background"). The background subtracted intensity values were plotted over time using Excel.

For recordings of YFP:: α -tubulin embryos with Calyculin A treatment, microscope and laser setup were used as detailed in Grill et al. (2003), but Metamorph software controlled the microscope. Worms were dissected in 10 μ l egg buffer (118 mM NaCl, 48 mM KCl, 2 mM CaCl₂, 2 mM MgCl₂, 25 mM HEPES, pH 7.3) on a polylysine (Sigma)-coated microscope slide. Calyculin A (Sigma) from a 1 mM stock in DMSO was added to a final concentration of 10 μ M; for controls, DMSO alone was added to 1% v/v. For each embryo, one control image was acquired at the start of metaphase, as determined by DIC optics, and entry of the drug was facilitated by targeting the embryonic eggshell with UV laser beam pulses.

Electron Tomography and 3D Modeling

Sample preparation for electron tomography was carried out essentially as published (Srayko et al., 2006). Briefly, isolated RNAi embryos were high-pressure frozen (Leica EMPACT2+RTS), freeze-substituted (Leica EM AFS), and thin-layer embedded in Epon/Araldite for serial sectioning. Electron tomography was performed on 300 nm plastic sections with a TECNAI F30 intermediate-voltage microscope (FEI) operated at 300 kV. Tomograms were computed and analyzed by using the IMOD software package as published (O'Toole et al., 2003).

Antibody Production

RSA-1 antibodies were generated by immunizing rabbits with the RSA-1 COOH-terminal peptide H₂N-AGFLSNSDDYMKYERREQ-COOH. This peptide with an additional N-terminal cysteine residue was used for coupling the peptide to SulfoLink resin (Pierce) for affinity purification of the antiserum. The antibody was directly labeled using Alexa Fluor 488 succinimidyl ester (Molecular Probes) according to the manufacturer's instructions.

Two different antibodies were generated against RSA-2. α RSA-2(pep) was obtained by immunizing rabbits with the peptide H₂N-CQMVLESEIDATVTDV-COOH (aa 933–947 plus aminoterminal cysteine) and affinity purification as described above. α RSA-2(M1522) was obtained by immunizing rabbits with a GST-RSA-2(aa 1–714) fragment and purification of the antiserum with MBP-RSA-2(aa 1–714). Purification of antisera was performed according to standard procedures (Harlow and Lane, 1988).

Immunoprecipitations

Immunoprecipitations were essentially performed as previously described (Desai et al., 2003). For RSA-1 IPs, whole worm extracts of transgenic worms expressing LAP::RSA-1 were used. LAP::RSA-1 was precipitated using an affinity purified antibody raised in goat against 6-His EGFP (protein expression and purification facility, MPI-CBG). For controls, rabbit random IgG (dianova) was incubated with extracts from LAP::RSA-1 worms or anti-6-His EGFP antibodies were incubated with wild-type extracts. Proteins were eluted in sample buffer and separated by SDS-PAGE. Mass spectrometric analysis of these samples was performed by nanoLC-MS-MS as described in the Supplemental Data.

For RSA-2 and TPXL-1 IPs, either α RSA-2(pep) or α TPXL-1(aa 1–210) (Ozlu et al., 2005) antibodies and 1 ml of *C. elegans* embryo extract were used. Proteins were eluted in sample buffer for Western blot analysis or in 50 mM Tris (pH 8.5), 8 M urea for mass spectrometry. Mass spectrometry on these samples was conducted essentially as described in Cheeseman et al. (2001), but tandem mass spectra were searched against the most recent version of the predicted *C. elegans* proteins (Wormpep150).

Western Blotting and Immunofluorescence

Extract preparation and Western blotting was performed as described (Ozlu et al., 2005). 100% input corresponded to four worms. For the detection of RSA-2, the α RSA-2(M1522) antibody was used at 0.3 μ g/ml. Immunofluorescence experiments were performed as described (Oegema et al., 2001). Antibodies were used at 1 μ g/ml. The Alexa 488 conjugated α RSA-1 antibody was used for labeling RSA-1. The α RSA-2(pep) antibody was used for detection of RSA-2 and "converted" to a goat antibody by incubation with an anti-goat F_{ab} fragment as described (Hannak et al., 2002). DM1 α (Sigma) was used at a dilution of 1:500 to visualize microtubules. The antibody against γ -tubulin has been described previously (Hannak et al., 2001). Z stacks through entire embryos were acquired using a wide-field Delta Vision microscope (Applied Precision). The stacks were computationally projected and deconvolved using SoftWorx (Applied Precision).

Yeast Two-Hybrid Analysis

For yeast two-hybrid assays, the Proquest Two-Hybrid System with Gateway Technology (Invitrogen) was used according to the manufacturer's instructions. The host strain for the analysis was MAV203 (MAT α , *leu2-3,112*, *trp1-901*, *his3 Δ 200*, *ade2-101*, *gal4 Δ* , *gal80 Δ* , *SPAL10::URA3*, *GAL1::lacZ*, *HIS3_{UAS}*, *GAL1::HIS3@LYS2*, *can1^R*, *cyh2^R*).

Briefly, a vector encoding RSA-2 fused to the DNA binding domain (BD) of the GAL4 transcription factor was cotransformed with GAL4 activating domain (AD) fusions of either full-length RSA-1 or a SPD-5 fragment that corresponded to aa 280–1198. This SPD-5 fragment was obtained in a separate yeast two-hybrid screen for interactors of RSA-2 (unpublished). Complex formation was detected by activation of the lacZ reporter gene in a β -galactosidase assay and growth on plates lacking either histidine or uracil (not shown). β -galactosidase units were quantified using ONPG as substrate according to the manufacturer's instruction. Values for β -galactosidase units as well as the vectors used are described in Table S1.

Supplemental Data

Supplemental Data include four figures, three tables, Supplemental Experimental Procedures, Supplemental References, and ten movies and can be found with this article online at <http://www.cell.com/cgi/content/full/128/1/115/DC1/>.

ACKNOWLEDGMENTS

We thank W. Zachariae for advice during the course of this study and for comments on the manuscript. Moreover, we thank all the members

of the Hyman Lab, especially C. Cowan, N. Ozlu, M. van Breugel, C. Hoege, and L. Pelletier for stimulating discussions and experimental advice. We are grateful to E. Cuppen (Hubrecht Laboratory, Utrecht, The Netherlands) for advice on the TILLING procedure, to S. Winkler and the MPI-CBG TILLING facility as well as to the MPI-CBG sequencing facility headed by G. Wiebe for excellent technical support in isolating the *rsa-1(dd13)* allele, to Thomas Döbel for help with modeling of EM tomograms, and to B. Habermann for help with bioinformatic analysis. We thank C. Cowan for *C. elegans* strains, M. Tipsword and M. Ruer for reagents, and M. Boxem (Dana-Farber Cancer Institute, Boston, MA) for sharing data prior to publication. We are grateful to the *Caenorhabditis elegans* Genetics Center for providing strains. We also thank C. Cowan, N. Ozlu, C. Hoege, and S. Schuck for comments on the manuscript.

Received: April 28, 2006

Revised: September 28, 2006

Accepted: October 20, 2006

Published: January 11, 2007

REFERENCES

- Andrews, P.D., Ovechkina, Y., Morrice, N., Wagenbach, M., Duncan, K., Wordeman, L., and Swedlow, J.R. (2004). Aurora B regulates MCAK at the mitotic centromere. *Dev. Cell* 6, 253–268.
- Arnold, H.K., and Sears, R.C. (2006). Protein phosphatase 2A regulatory subunit B56{alpha} associates with c-myc and negatively regulates c-myc accumulation. *Mol. Cell. Biol.* 26, 2832–2844.
- Brenner, S. (1974). The genetics of *Caenorhabditis elegans*. *Genetics* 77, 71–94.
- Camilleri, C., Azimzadeh, J., Pastuglia, M., Bellini, C., Grandjean, O., and Bouchez, D. (2002). The Arabidopsis TONNEAU2 gene encodes a putative novel protein phosphatase 2A regulatory subunit essential for the control of the cortical cytoskeleton. *Plant Cell* 14, 833–845.
- Carmena, M., and Earnshaw, W.C. (2003). The cellular geography of aurora kinases. *Nat. Rev. Mol. Cell Biol.* 4, 842–854.
- Cassimeris, L. (1999). Accessory protein regulation of microtubule dynamics throughout the cell cycle. *Curr. Opin. Cell Biol.* 11, 134–141.
- Cassimeris, L., and Spittle, C. (2001). Regulation of microtubule-associated proteins. *Int. Rev. Cytol.* 210, 163–226.
- Cheeseman, I.M., Brew, C., Wolyniak, M., Desai, A., Anderson, S., Muster, N., Yates, J.R., Huffaker, T.C., Drubin, D.G., and Barnes, G. (2001). Implication of a novel multiprotein Dam1p complex in outer kinetochore function. *J. Cell Biol.* 155, 1137–1145.
- Dagda, R.K., Zausa, J.A., Wadzinski, B.E., and Strack, S. (2003). A developmentally regulated, neuron-specific splice variant of the variable subunit Bbeta targets protein phosphatase 2A to mitochondria and modulates apoptosis. *J. Biol. Chem.* 278, 24976–24985.
- Dammermann, A., Muller-Reichert, T., Pelletier, L., Habermann, B., Desai, A., and Oegema, K. (2004). Centriole assembly requires both centriolar and pericentriolar material proteins. *Dev. Cell* 7, 815–829.
- Desai, A., and Mitchison, T.J. (1997). Microtubule polymerization dynamics. *Annu. Rev. Cell Dev. Biol.* 13, 83–117.
- Desai, A., Verma, S., Mitchison, T.J., and Walczak, C.E. (1999). Kin I kinesins are microtubule-destabilizing enzymes. *Cell* 96, 69–78.
- Desai, A., Rybina, S., Muller-Reichert, T., Shevchenko, A., Hyman, A., and Oegema, K. (2003). KNL-1 directs assembly of the microtubule-binding interface of the kinetochore in *C. elegans*. *Genes Dev.* 17, 2421–2435.
- Faux, M.C., and Scott, J.D. (1996). More on target with protein phosphorylation: conferring specificity by location. *Trends Biochem. Sci.* 21, 312–315.
- Gliksman, N.R., Parsons, S.F., and Salmon, E.D. (1992). Okadaic acid induces interphase to mitotic-like microtubule dynamic instability by inactivating rescue. *J. Cell Biol.* 119, 1271–1276.
- Grill, S.W., Gonczy, P., Stelzer, E.H., and Hyman, A.A. (2001). Polarity controls forces governing asymmetric spindle positioning in the *Caenorhabditis elegans* embryo. *Nature* 409, 630–633.
- Grill, S.W., Howard, J., Schaffer, E., Stelzer, E.H., and Hyman, A.A. (2003). The distribution of active force generators controls mitotic spindle position. *Science* 301, 518–521.
- Gruss, O.J., and Vernos, I. (2004). The mechanism of spindle assembly: functions of Ran and its target TPX2. *J. Cell Biol.* 166, 949–955.
- Hamill, D.R., Severson, A.F., Carter, J.C., and Bowerman, B. (2002). Centrosome maturation and mitotic spindle assembly in *C. elegans* require SPD-5, a protein with multiple coiled-coil domains. *Dev. Cell* 3, 673–684.
- Hannak, E., Kirkham, M., Hyman, A.A., and Oegema, K. (2001). Aurora-A kinase is required for centrosome maturation in *Caenorhabditis elegans*. *J. Cell Biol.* 155, 1109–1116.
- Hannak, E., Oegema, K., Kirkham, M., Gonczy, P., Habermann, B., and Hyman, A.A. (2002). The kinetically dominant assembly pathway for centrosomal asters in *Caenorhabditis elegans* is gamma-tubulin dependent. *J. Cell Biol.* 157, 591–602.
- Harlow, E., and Lane, D. (1988). *Antibodies: A Laboratory Manual* (Cold Spring Harbor, NY: Cold Spring Harbor Press).
- Janssens, V., and Goris, J. (2001). Protein phosphatase 2A: a highly regulated family of serine/threonine phosphatases implicated in cell growth and signalling. *Biochem. J.* 353, 417–439.
- Kao, G., Tuck, S., Baillie, D., and Sundaram, M.V. (2004). *C. elegans* SUR-6/PR55 cooperates with LET-92/protein phosphatase 2A and promotes Raf activity independently of inhibitory Akt phosphorylation sites. *Development* 131, 755–765.
- Karsenti, E., and Vernos, I. (2001). The mitotic spindle: a self-made machine. *Science* 294, 543–547.
- Kinoshita, K., Noetzel, T.L., Pelletier, L., Mechtler, K., Drechsel, D.N., Schwager, A., Lee, M., Raff, J.W., and Hyman, A.A. (2005). Aurora A phosphorylation of TACC3/maskin is required for centrosome-dependent microtubule assembly in mitosis. *J. Cell Biol.* 170, 1047–1055.
- Lan, W., Zhang, X., Klime-Smith, S.L., Rosasco, S.E., Barrett-Wilt, G.A., Shabanowitz, J., Hunt, D.F., Walczak, C.E., and Stukenberg, P.T. (2004). Aurora B phosphorylates centromeric MCAK and regulates its localization and microtubule depolymerization activity. *Curr. Biol.* 14, 273–286.
- Nigg, E.A. (2001). Mitotic kinases as regulators of cell division and its checkpoints. *Nat. Rev. Mol. Cell Biol.* 2, 21–32.
- Oegema, K., Desai, A., Rybina, S., Kirkham, M., and Hyman, A.A. (2001). Functional analysis of kinetochore assembly in *Caenorhabditis elegans*. *J. Cell Biol.* 153, 1209–1226.
- Oegema, K., and Hyman, T. (2006). *WormBook*, ed. The *C. elegans* Research Community (*WormBook*) 10.1895/wormbook.1.72.1, <http://www.wormbook.org>.
- O'Toole, E.T., McDonald, K.L., Mäntler, J., McIntosh, J.R., Hyman, A.A., and Müller-Reichert, T. (2003). Morphologically distinct microtubule ends in the mitotic centrosome of *Caenorhabditis elegans*. *J. Cell Biol.* 163, 451–456.
- Ohi, R., Sapra, T., Howard, J., and Mitchison, T.J. (2004). Differentiation of cytoplasmic and meiotic spindle assembly MCAK functions by Aurora B-dependent phosphorylation. *Mol. Biol. Cell* 15, 2895–2906.
- Ozlu, N., Srayko, M., Kinoshita, K., Habermann, B., O'Toole, E.T., Muller-Reichert, T., Schmalz, N., Desai, A., and Hyman, A.A. (2005). An essential function of the *C. elegans* ortholog of TPX2 is to localize activated aurora A kinase to mitotic spindles. *Dev. Cell* 9, 237–248.

- Praitis, V., Casey, E., Collar, D., and Austin, J. (2001). Creation of low-copy integrated transgenic lines in *Caenorhabditis elegans*. *Genetics* 157, 1217–1226.
- Siddiqui, S.S. (2002). Metazoan motor models: kinesin superfamily in *C. elegans*. *Traffic* 3, 20–28.
- Sonnichsen, B., Koski, L.B., Walsh, A., Marschall, P., Neumann, B., Brehm, M., Alleaume, A.M., Artelt, J., Bettencourt, P., Cassin, E., et al. (2005). Full-genome RNAi profiling of early embryogenesis in *Caenorhabditis elegans*. *Nature* 434, 462–469.
- Sontag, E., Nunbhakdi-Craig, V., Bloom, G.S., and Mumby, M.C. (1995). A novel pool of protein phosphatase 2A is associated with microtubules and is regulated during the cell cycle. *J. Cell Biol.* 128, 1131–1144.
- Srayko, M., Kaya, A., Stamford, J., and Hyman, A.A. (2005). Identification and characterization of factors required for microtubule growth and nucleation in the early *C. elegans* embryo. *Dev. Cell* 9, 223–236.
- Srayko, M., O'Toole, E.T., Hyman, A.A., and Müller-Reichert, T. (2006). Katanin disrupts the microtubule lattice and increases polymer number in *C. elegans* meiosis. *Curr. Biol.* 19, 1944–1949.
- Stemple, D.L. (2004). TILLING—a high-throughput harvest for functional genomics. *Nat. Rev. Genet.* 5, 145–150.
- Sumiyoshi, E., Sugimoto, A., and Yamamoto, M. (2002). Protein phosphatase 4 is required for centrosome maturation in mitosis and sperm meiosis in *C. elegans*. *J. Cell Sci.* 115, 1403–1410.
- Tournebize, R., Andersen, S.S., Verde, F., Doree, M., Karsenti, E., and Hyman, A.A. (1997). Distinct roles of PP1 and PP2A-like phosphatases in control of microtubule dynamics during mitosis. *EMBO J.* 16, 5537–5549.
- Verde, F., Labbe, J.C., Doree, M., and Karsenti, E. (1990). Regulation of microtubule dynamics by *cdc2* protein kinase in cell-free extracts of *Xenopus* eggs. *Nature* 343, 233–238.
- Wittmann, T., Hyman, A., and Desai, A. (2001). The spindle: a dynamic assembly of microtubules and motors. *Nat. Cell Biol.* 3, E28–E34.